
Disentangling Factors of Variation Using Few Labels

Francesco Locatello^{2,4}, Michael Tschannen³, Stefan Bauer⁴, Gunnar Rätsch², Bernhard Schölkopf⁴,
and Olivier Bachem¹

¹Google Research, Brain Team

²Dept. of Computer Science, ETH Zurich

³Dept. of Information Technology and Electrical Engineering, ETH Zurich

⁴Max-Planck Institute for Intelligent Systems

Abstract

Learning disentangled representations is considered a cornerstone problem in representation learning. Recently, Locatello et al. (2019) demonstrated that unsupervised disentanglement learning without inductive biases is theoretically impossible and that existing inductive biases and unsupervised methods do not allow to consistently learn disentangled representations. However, in many practical settings, one might have access to a very limited amount of supervision, for example through manual labeling of training examples. In this paper, we investigate the impact of such supervision on state-of-the-art disentanglement methods and perform a large scale study, training over 29 000 models under well-defined and reproducible experimental conditions. We first observe that a very limited number of labeled examples (0.01–0.5% of the data set) is sufficient to perform model selection on state-of-the-art unsupervised models. Yet, if one has access to labels for supervised model selection, this raises the natural question of whether they should also be incorporated into the training process. As a case-study, we test the benefit of introducing (very limited) supervision into existing state-of-the-art unsupervised disentanglement methods exploiting both the values of the labels and the ordinal information that can be deduced from them. Overall, we empirically validate that with very little and potentially imprecise supervision it is possible to reliably learn disentangled representations.

1 Introduction

In machine learning, it is commonly assumed that high-dimensional observations \mathbf{x} (such as images) are the manifestation of a low-dimensional latent variable \mathbf{z} of ground-truth factors of variation [2, 35, 7, 62]. More specifically, one often assumes that there is a distribution $p(\mathbf{z})$ over these latent variables and that observations in this ground-truth model are first generated by sampling \mathbf{z} from $p(\mathbf{z})$ and that the observations \mathbf{x} are then sampled from a conditional distribution $p(\mathbf{x}|\mathbf{z})$. The goal of disentanglement learning is to find a representation of the data $r(\mathbf{x})$ which captures all the ground-truth factors of variation in \mathbf{z} independently. The hope is that such representations will be interpretable, maximally compact, allow for counterfactual reasoning and be useful for a large variety of downstream task [2, 49, 39, 3, 56, 37, 17, 41, 62, 19, 60]. In particular, we hope to learn a disentangled representation with as little supervision as possible so that all the available labels can be used to learn downstream tasks [2, 57, 49, 48, 58].

Current state-of-the-art unsupervised disentanglement approaches enrich the *Variational Autoencoder* (VAE) [33] objective with different unsupervised regularizers that aim to encourage disentangled representations [20, 5, 31, 6, 36, 54, 44, 53]. While these approaches can find disentangled representations if one trains a lot of different models, there is a large variance across these models and it appears hard to identify the ones with disentangled representations without supervision [42].

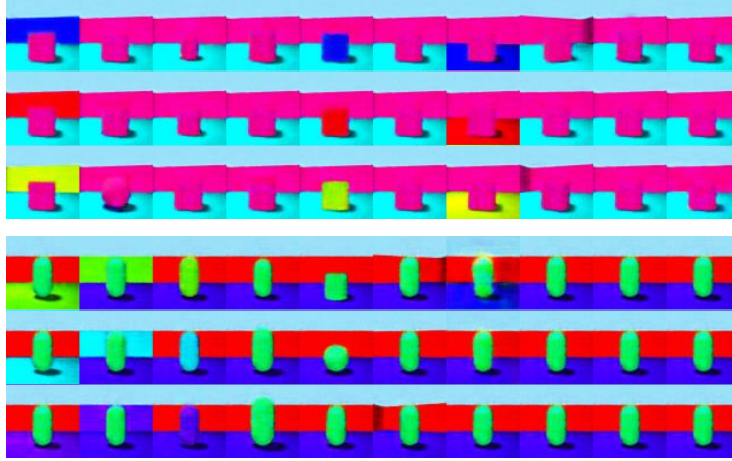


Figure 1: Latent traversals (each column corresponds to a different latent variable being varied) on Shapes3D for the β -TCVAE model with best validation MIG (top) and for the semi-supervised β -TCVAE model with best validation loss (bottom), both using only 1000 labeled examples for validation and/or supervision.

This is consistent with the theoretical result of [42] that the unsupervised learning of disentangled representations is impossible without inductive biases.

While visual inspection can be used to select good model runs and hyperparameters, we argue that such supervision should be made explicit. We hence consider the practically realistic setting where one has access to labels for the latent variables \mathbf{z} for a very limited number of observations \mathbf{x} , for example through human labeling. Even though this setting is not universally applicable (e.g. when the observations are not human interpretable or the ground-truth factors are unknown), we argue that it is broad enough to warrant investigation. Furthermore, while the true ground-truth model may be unknown and non-unique [42], the considered setting allows us to encode additional knowledge and implicit biases into the learned representation via the labels.

In this paper, we first investigate whether access to limited labels allows us to reliably perform model selection of current state-of-the-art unsupervised disentanglement methods. Second, we explore whether it is more beneficial to incorporate the limited amount of labels into training. For this purpose, we perform a reproducible large scale experimental study¹, training over 29 000 models on four different data sets. We found that unsupervised training with supervised validation enables reliable learning of disentangled representations. On the other hand, using some of the labeled data for training is beneficial both in terms of disentanglement and downstream performance. Overall, we show that a very small amount of supervision is enough to learn disentangled representations as illustrated in Figure 1. Our key contributions can be summarized as follows:

- We observe that some of the existing disentanglement metrics (which require observations of \mathbf{z}) can be used to tune the hyperparameters of unsupervised methods even when only very few labeled examples are available (Section 3). Therefore, training a large number of models and introducing supervision to select the good runs is a viable solution to overcome the impossibility result of [42].
- We find that adding a simple supervised loss, using as little as 100 labeled examples, outperforms unsupervised training with supervised model validation both in terms of disentanglement scores and downstream performance (Section 4.2). Further, the inductive bias given by the ordinal information of the factors of variation is shown to be useful for learning disentangled representations (Section 4.4). This result empirically validates the importance of inductive biases in disentanglement learning as theoretically claimed in [42, 62].
- We discover that both unsupervised training with supervised validation and semi-supervised training do not need precise labels, but imprecise approximations are sufficient (Sections 3.2 and 4.3). Furthermore, binning may have a regularizing effect and can improve the robustness of certain metrics when only very few labels are available.

¹Reproducing these experiment requires approximately 4.73 GPU years (NVIDIA P100).

2 Background and related work

Consider a generative model with latent variable \mathbf{z} with factorized density $p(\mathbf{z}) = \prod_{i=1}^d p(z_i)$, where $d > 1$, and observations \mathbf{x} obtained as samples from $p(\mathbf{x}|\mathbf{z})$. Intuitively, the goal of disentanglement learning is to find a representation $r(\mathbf{x})$ separating the factors of variation into independent components so that a change in a dimension of \mathbf{z} corresponds to a change in a dimension of $r(\mathbf{x})$ [2]. Refinements of this definition include disentangling independent groups in the topological sense [19] and learning disentangled causal models [60]. These definitions are reflected in various disentanglement metrics that aim at measuring some structural property of the statistical dependencies between \mathbf{z} and $r(\mathbf{x})$.

The *BetaVAE* score [20] measures disentanglement as the accuracy of a linear classifier that predicts the index of a fixed factor of variation. The *FactorVAE* score [31] replaces the linear classifier of the BetaVAE score with a majority vote classifier on the relative variance of each dimension of $r(\mathbf{x})$ when a dimension of \mathbf{z} is fixed. The *Mutual Information Gap (MIG)* [6] computes for each dimension z_i of \mathbf{z} the normalized gap in mutual information between the coordinate of $r(\mathbf{x})$ with the highest and second highest mutual information with z_i . The *Modularity* [52] computes the mutual information between each coordinate of \mathbf{z} and $r(\mathbf{x})$ and measures if each dimension of $r(\mathbf{x})$ depends on at most one factor of variation. The Disentanglement metric of [14] (which we call *DCI Disentanglement* following [42]) computes disentanglement based on the entropy of the feature importance (quantified e.g. via random forest) of each dimension of $r(\mathbf{x})$ for predicting \mathbf{z} . Finally, the *SAP score* [36] trains a classifier on each dimension of $r(\mathbf{x})$ predicting each dimension of \mathbf{z} and then computes the average gap in the prediction error of the two most predictive latent dimensions for each factor.

Since all these metrics require access to labels \mathbf{z} they cannot be used for unsupervised training. Many state-of-the-art unsupervised disentanglement methods therefore extend VAEs [33] with a regularizer $R_u(q_\phi(\mathbf{z}|\mathbf{x}))$ that enforces structure in the latent space of the VAE induced by the encoding distribution $q_\phi(\mathbf{z}|\mathbf{x})$ with the hope that this leads to disentangled representations. These approaches [20, 5, 31, 6, 36] can be cast under the following optimization template:

$$\max_{\phi, \theta} \underbrace{\mathbb{E}_{\mathbf{x}}[\mathbb{E}_{q_\phi(\mathbf{z}|\mathbf{x})}[\log p_\theta(\mathbf{x}|\mathbf{z})] - D_{\text{KL}}(q_\phi(\mathbf{z}|\mathbf{x})||p(\mathbf{z}))]}_{=:\text{ELBO}(\phi, \theta)} + \beta \mathbb{E}_{\mathbf{x}}[R_u(q_\phi(\mathbf{z}|\mathbf{x}))]. \quad (1)$$

The β -VAE [20] and AnnealedVAE [5] reduce the capacity of the VAE bottleneck under the assumption that encoding the factors of variation is the most efficient way to achieve a good reconstruction [49]. The Factor-VAE [31] and β -TCVAE both penalize the total correlation of the aggregated posterior $q(\mathbf{z})$ (i.e. the encoder distribution after marginalizing the training data). The DIP-VAE variants [36] match the moments of the aggregated posterior and a factorized distribution. We refer to Appendix B of [42] and Section 3 of [62] for a more detailed description of these regularizers.

While there has also been work on semi-supervised disentanglement learning [50, 8, 45, 47, 32, 34], these methods aim to disentangle only *some* observed factors of variation from the other latent variables which themselves remain entangled. Furthermore, if the observed factors of variation and the observations are confounded by a latent variable, the structure is known to not be identifiable [49, 11, 60]. In contrast, we consider the setting where one has access an extremely limited number of fully labeled observations (\mathbf{x}, \mathbf{z}) and a large number of unlabeled observations of \mathbf{x} . Exploiting relational information or knowledge of the effect of the factors of variation have both been qualitatively studied to learn disentangled representations [23, 9, 30, 18, 63, 16, 13, 25, 65, 43, 35, 55, 4]. These are not limiting assumption especially for sequential data or reinforcement learning [61, 59, 38, 46, 21, 22]. However, most of these works did not quantitatively measure disentanglement as they see disentanglement as tool to achieve some downstream goal. While a quantitative comparison of these methods in terms of disentanglement and sample complexity is an interesting research direction, it is beyond the scope of this paper.

Other related work. Due to the lack of a commonly accepted formal definition, the term “disentangled representations” has been used in very different lines of work. There is for example a rich literature in disentangling pose from content in 3D objects and content from motion in videos [64, 65, 24, 15, 12, 18, 26]. This can be achieved with different degrees of supervision, ranging from fully unsupervised to semi-supervised. Another line of work aims at disentangling class labels from latent variables by assuming the existence of a causal model where the latent variable \mathbf{z} has an arbitrary factorization with the class variable \mathbf{y} . In this setting, \mathbf{y} is partially observed [50, 8, 45, 47, 32, 34].

Without further assumptions on the structure of the graphical model, this is equivalent to partially observed factors of variation with latent confounders. Except for very special cases, the recovery of the structure of the generative model is known to be impossible with purely observational data [49, 11, 60]. Here, we intend to disentangle factors of variation in the sense of [2, 60, 19]. We aim at separating the effects of all factors of variation, which translates to learning a representation with independent components. This problem has already been studied extensively in the non-linear ICA literature [10, 1, 29, 26, 27, 28], therefore the impossibility result of [42] may not be surprising.

3 Unsupervised training with supervised model selection

The impossibility result of [42] states that for a factorized prior $p(\mathbf{z})$ one can construct infinitely many generative models all entangled with each other. This implies that there are many equally plausible generative models and an unsupervised method cannot distinguish between them without further inductive biases. While state-of-the-art unsupervised model can find disentangled representations, there is a large variance in the disentanglement of representations when different random seeds are used. At the same time, it appears hard to identify well-disentangled models in a purely unsupervised fashion [42].

In this section, we investigate whether commonly used disentanglement metrics can be used to identify good models if we have a very small number of labeled observations available. While existing metrics are often evaluated using as much as 10 000 labeled examples, it might be feasible in many practical settings to annotate 100 or 1000 data points and use them to obtain a disentangled representation. At the same time, it is unclear whether such an approach would work as existing disentanglement metrics have been found to be noisy (even with more samples) [31]. Finally, we explicitly note that the impossibility result of [42] does not apply in this setting as we do observe samples from \mathbf{z} .

3.1 Experimental setup

Data sets. We consider four commonly used disentanglement data sets where one has explicit access to the ground-truth generative model and the factors of variation: *dSprites* [20], *Cars3D* [51], *SmallNORB* [40] and *Shapes3D* [31]. Following [42], we consider the statistical setting where one directly samples from the generative model, effectively side-stepping the issue of empirical risk minimization and overfitting. For each data set, we assume to have either 100 or 1000 labeled examples available and a large amount of unlabeled observations. We note that 100 labels correspond to labeling 0.01% of the state space of *dSprites*, 0.5% of *Cars3D*, 0.4% of *SmallNORB* and 0.02% of *Shapes3D*.

True vs. imprecise labels. In addition to using the true labels of the ground-truth generative model, we also consider the setting where the returned labels are binned to take at most five different values. This is meant to simulate the process of a practitioner quickly labeling a small number of images.

Model selection metrics. We use MIG [6], DCI Disentanglement [14] and SAP score [36] for model selection as they can be used on purely observational data. In contrast, the BetaVAE [20] and FactorVAE [31] scores cannot be used for model selection on observational data because they require access to the true generative model and the ability to perform interventions. At the same time, prior work has found all these disentanglement metrics to be substantially correlated [42].

Experimental protocol. In total, we consider 16 different experimental settings where an experimental setting corresponds to a data set (*dSprites/Cars3D/SmallNORB/Shapes3D*), a specific number of labeled examples (100/1000), and a labeling setting (perfect/imprecise). For each considered setting, we generate five different sets of labeled examples using five different random seeds. For each of these labeled sets, we train cohorts of β -VAEs [20], β -TCVAEs [6], Factor-VAEs [31], and DIP-VAE-Is [36] where each model cohort consists of 36 different models with 6 different hyperparameters for each model and 6 random seeds. For a detailed description of hyperparameters, architecture, and model training we refer to Section A. For each of these 11 520 models, we then compute all the model selection metrics on the set of labeled examples and use these scores to select the best models in each of the cohorts. We attach as a prefix *U/S* for *unsupervised* training with *supervised* model selection. Finally, we evaluate robust estimates of the BetaVAE score, the FactorVAE score, MIG, Modularity, DCI disentanglement and SAP score for each model based on an additional evaluation set of 10 000 samples² in the same way as in [42].

²For the BetaVAE score and the FactorVAE score, this includes specific realizations based on interventions on the latent space.

	Dataset = dSprites							Dataset = dSprites					
MIG (MS100)	81	67	92	92	-0	67	MIG (MS1000)	84	76	99	94	-4	70
SAP (MS100)	17	14	18	18	0	17	SAP (MS1000)	66	50	70	69	-3	69
DCI (MS100)	79	68	88	94	-1	59	DCI (MS1000)	84	75	93	99	-4	63
	(A)	(B)	(C)	(D)	(E)	(F)		(A)	(B)	(C)	(D)	(E)	(F)

Figure 2: Rank correlation of validation metrics computed with 100 examples (left) and 1000 examples (right) and test metrics on dSprites. Legend: (A)=BetaVAE Score, (B)=FactorVAE Score, (C)=MIG, (D)=DCI Disentanglement, (E)=Modularity, (F)=SAP.

3.2 Key findings

We highlight our key findings with plots picked to be representative of our main results. In Appendices B-C, we provide complete sets of plots for different methods, data sets and disentanglement metrics.

Dataset = dSprites						
MIG (MS100)	77	78	94	90	-14	57
SAP (MS100)	30	25	32	32	-0	22
DCI (MS100)	78	79	92	94	-13	54
	(A)	(B)	(C)	(D)	(E)	(F)
Dataset = dSprites						
MIG (MS1000)	83	81	98	91	-4	65
SAP (MS1000)	75	71	86	82	-2	59
DCI (MS1000)	83	82	94	98	-6	60
	(A)	(B)	(C)	(D)	(E)	(F)

Figure 3: Rank correlation of validation metrics and test metrics. Validation metrics are computed with 100 (top) and 1000 (bottom) examples with *labels binned to five categories*. Legend: (A)=BetaVAE Score, (B)=FactorVAE Score, (C)=MIG, (D)=DCI Disentanglement, (E)=Modularity, (F)=SAP.

Model selection with perfect labels. In Figure 2 (left), we show the rank correlation between the validation metrics computed on 100 samples and the test metrics on dSprites. We observe that MIG and DCI Disentanglement generally correlate well with the test metrics (with the only exception of Modularity) while the correlation for the SAP score is substantially lower. This is not surprising given that the SAP score requires us to train a multiclass support vector machine for each dimension of $r(\mathbf{x})$ predicting each dimension of \mathbf{z} . For example, on Cars3D the factor determining the object type can take 183 distinct values which can make it hard to train a classifier using only 100 training samples. In Figure 2 (right), we observe that the rank correlation improves considerably for the SAP score if we have 1000 labeled examples available and slightly for MIG and DCI Disentanglement. In Figure 1 we show latent traversals for the U/S model achieving maximum validation MIG on 1000 examples on Shapes3D.

Model selection with imperfect labels. Figure 3 shows the rank correlation between the model selection metrics with binned values and the test metrics with exact labels. We observe that the metrics are surprisingly robust with respect to binned labels and they still correlate well with the test metrics. This is meant to simulate the process of a practitioner labeling by hand a reasonable amount of images into “rough” categories. We observe that the rough labeling does not seem detrimental to the performance of the model selection with few labels. We interpret these results as that for the purpose of disentanglement, fine-grained labeling is not critical as the different factors of variation can already be disentangled using coarse feedback. Interestingly, the rank correlation of the SAP score and the test metrics improves significantly (in particular for a 100 labels). This is to be expected, as now we only have five classes for each factor of variation so the classification problem becomes easier and the estimate of the SAP score more reliable.

Conclusions: From this experiment, we conclude that it is possible to identify good runs and hyperparameter settings on the considered data sets using the MIG and the DCI Disentanglement based on 100 labeled examples. The SAP score may also be used, depending on how difficult the underlying classification problem is. Surprisingly, these metrics are reliable even if we do not collect the labels exactly but only use imprecise labels for the factors of variation \mathbf{z} . We conclude that labeling a small number of examples for supervised validation appears to be a reasonable solution to learn disentangled representations in practice.

4 Incorporating label information during training

Using labels for model selection—even only a small amount—raises the natural question whether these labels should rather be used for training a good model directly. In particular, such an approach also allows structure of the ground-truth factors of variation to be used, for example ordinal information. In this section, we investigate a simple approach to incorporate the information of very few labels into existing unsupervised disentanglement methods and compare that approach to the alternative of unsupervised training with supervised model selection (as described in Section 3).

The key idea is that the limited labeling information should be used to ensure a latent space of the VAE with desirable structure with respect to the ground-truth factors of variation (as there is not enough labeled samples to learn a good representation solely from the labels). We hence incorporate supervision by constraining Equation 1:

$$\max_{\phi, \theta} \quad \text{ELBO}(\phi, \theta) + \beta \mathbb{E}_{\mathbf{x}} R_u(q_\phi(\mathbf{z}|\mathbf{x})). \quad (2)$$

$$\text{s.t.} \quad \mathbb{E}_{\mathbf{x}, \mathbf{z}} R_s(q_\phi(\mathbf{z}|\mathbf{x}), \mathbf{z}) \leq \kappa$$

where $R_s(q_\phi(\mathbf{z}|\mathbf{x}), \mathbf{z})$ is a function computed on the (few) available observation-label pairs and where $\kappa > 0$ is a threshold. In other words, we constrain the otherwise unsupervised problem using some supervised penalty. We can now include R_s into the loss as a regularizer under the Karush-Kuhn-Tucker conditions:

$$\max_{\phi, \theta} \quad \text{ELBO}(\phi, \theta) + \beta \mathbb{E}_{\mathbf{x}} R_u(q_\phi(\mathbf{z}|\mathbf{x})) + \gamma_{sup} \mathbb{E}_{\mathbf{x}, \mathbf{z}} R_s(q_\phi(\mathbf{z}|\mathbf{x}), \mathbf{z}). \quad (3)$$

We rely on the binary cross-entropy loss to match the factors to their targets, i.e., $R_s(q_\phi(\mathbf{z}|\mathbf{x}), \mathbf{z}) = -\sum_{i=1}^d z_i \log(\sigma(r(\mathbf{x})_i)) + (1 - z_i) \log(1 - \sigma(r(\mathbf{x})_i))$, where the targets z_i are normalized to $[0, 1]$, $\sigma(\cdot)$ is the logistic function and $r(\mathbf{x})$ corresponds to the mean (vector) of $q_\phi(\mathbf{z}|\mathbf{x})$. When \mathbf{z} has more dimensions than the number of factors of variation, only the first d dimensions are regularized where d is the number of factors of variation. While the z_i do not model probabilities of a binary random variable but factors of variation with potentially more than two discrete states, we have found the binary cross-entropy loss to work empirically well out-of-the-box. We also experimented with a simple L_2 loss $\|\sigma(r(\mathbf{x})) - \mathbf{z}\|^2$ for R_s , but obtained significantly worse results than for the binary cross-entropy. Similar observations were made in the context of VAEs where the binary cross-entropy as reconstruction loss is widely used and outperforms the L_2 loss even when pixels have continuous values in $[0, 1]$ (see, e.g. the code accompanying [6, 42]). Many other candidates for supervised regularizers could be explored in future work. However, given the already extensive experiments in this study, this is beyond the scope of this paper.

Inductive bias based on ordinal information. We emphasize that the considered supervised regularizer R_s uses an inductive bias in the sense that it assumes the ordering of the factors of variation to matter. This inductive bias is valid for many ground truth factors of variation both in the considered data sets and the real world (such as spatial positions, sizes, angles or even color). We argue that such inductive biases should generally be exploited whenever they are available which is the case if we have few manually annotated labels. To better understand role of ordinal information, we also investigate what happens if this inductive bias is removed (see next Section).

Differences to prior work on semi-supervised disentanglement. Existing semi-supervised approaches tackle the different problem of disentangling some factors of variation that are (partially) observed from the others that remain entangled [50, 8, 45, 47, 32]. In contrast, we assume to observe all ground-truth generative factors but only for a very limited number of observations. Disentangling only some of the factors of variation from the others is an interesting extension of this study. However, it is not clear how to adapt existing disentanglement scores to this different setup as they are designed to measure the disentanglement of *all* the factors of variation. We remark that the goal of this comparison is to test the two different approaches to incorporate supervision into state-of-the-art unsupervised disentanglement methods. Furthermore, by assuming to partially observe all the causal parents of \mathbf{x} we avoid unobserved confounding between \mathbf{z} and \mathbf{x} which makes the structure not identifiable from observational data [49, 11, 60]. For this reason, we resorted to a simple and well understood setup and supervised loss.

4.1 Experimental setup

True vs. imprecise labels vs. violation of inductive bias. In addition to using the true and binned labels of the ground-truth generative model, we also consider the case in which the ordinal information we deduce from the labeling is incorrect. In principle, this should not harm the performance on the test metrics as they are invariant to permutations of the ordinal information. Nevertheless, the supervised approach we consider explicitly make use of this ordinal information as inductive bias. This experiment is meant to showcase the importance of being explicit about the biases of the model as their violation might significantly harm performance.

Experimental protocol. To include supervision during training we split the labeled data set in a 90%/10% train/validation split. We consider 24 different experimental setting corresponding to a data set (*dSprites/Cars3D/SmallNORB/Shapes3D*), a specific number of labeled examples (100/1000), and a labeling setting (perfect/imprecise/randomly permuted). For each considered setting, we generate the same five different sets of labeled examples we used for the U/S models. For each of the labeled sets, we train cohorts of β -VAEs, β -TCVAEs, Factor-VAEs, and DIP-VAE-Is with the additional supervised regularizer $R_s(q_\phi(\mathbf{z}|\mathbf{x}), \mathbf{z})$. Each model cohort consists of 36 different models with 6 different hyperparameters for each of the two regularizers and one random seed. Details on the hyperparameter values can be found in Section A. For each of these 17 280 models, we compute the value of R_s on the validation examples and use these scores to select the best method in each of the cohorts. For these models we use the prefix S^2/S for *semi-supervised* training with *supervised* model selection and compute the same test disentanglement metrics as in Section 3.

Fully supervised baseline. We further consider a fully supervised baseline where the encoder is trained solely based on the supervised loss (without any decoder, KL divergence and reconstruction loss) with perfectly labeled training examples (again with a 90%/10% train validation split). The supervised loss does not have any tunable hyperparameters, and for each labeled data set, we run cohorts of six models with different random seeds. For each of these 240 models, we compute the value of R_s on the validation examples and use these scores to select the best method in the cohort.

4.2 Should labels be used for training?

First, we investigate the benefit of including the label information during training by comparing semi-supervised training with supervised validation in Figure 4 (left). Each dot in the plot corresponds to the median of the DCI Disentanglement score across the draws of the labeled subset on SmallNORB (using 100 vs 1000 examples for validation). For the U/S models we use MIG for validation (MIG has a higher rank correlation with most of the testing metric than other validation metrics, see Figure 2). From this plot one can see that the fully supervised baseline performs worse than the ones that make use of unsupervised data. As expected, having more labels can improve the median performance for the S^2/S approaches (depending on the data set and the test metric) but does not improve the U/S approaches (recall that we observed in Figure 2 (left) that the validation metrics already perform well with 100 samples).

To test whether incorporating the label information during training is better than using it for validation only, we report in Figure 6 (left) how often each approach outperforms all the others on a random disentanglement metric and data set. We observe that semi-supervised training often outperforms supervised validation. In particular, S^2/S - β -TC-VAE seem to improve the most, outperforming the S^2/S -DIP-VAE-I which was the best method for 100 labeled examples. Using 100 labeled examples, the S^2/S approach already wins in 70.5% of the trials. In Appendix C, we observe similar trends even when we use the testing metrics for validation (based on the full testing set) in the U/S models. The S^2/S approach seem to overall improve training and to transfer well across the different disentanglement metrics. In Figure 1 we show the latent traversals for the best S^2/S β -TCVAE using 1000 labeled examples. We observe that it achieves excellent disentanglement and that the unnecessary dimensions of the latent space are unused, as desired.

In their Figure 27, [42] showed that increasing regularization in unsupervised methods does not imply that the matrix holding the mutual information between all pairs of entries of $r(\mathbf{x})$ becomes closer to diagonal (which can be seen as a proxy for improved disentanglement). For the semi-supervised approach, in contrast, we observe in Figure 4 (center) that this is actually the case.

Finally, we study the effect of semi-supervised training on the (natural) downstream task of predicting the ground-truth factors of variation from the latent representation. We use four different training set

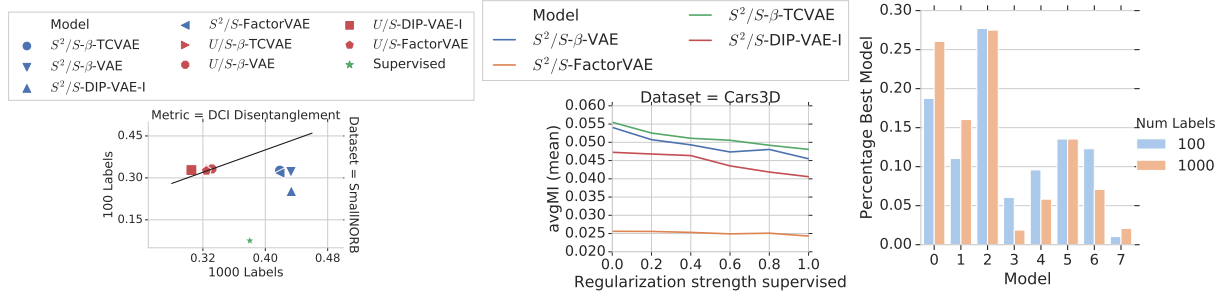


Figure 4: (left) Median across the draws of the labeled data set of the DCI Disentanglement test score on SmallNORB after validation with 100 and 1000 labeled examples. U/S were validated with the MIG. (center) Increasing the supervised regularization strength makes the matrix of pairwise mutual information $I(\mathbf{z}, r(\mathbf{x}))$ closer to diagonal. (right) Probability of each method being the best on a random downstream task. Legend: 0= S^2/S - β -TCVAE, 1= S^2/S - β -VAE, 2= S^2/S -DIP-VAE-I, 3= S^2/S -FactorVAE, 4= U/S - β -TCVAE, 5= U/S - β -VAE, 6= U/S -DIP-VAE-I, 7= U/S -FactorVAE. For the U/S methods we sample the validation metric uniformly.

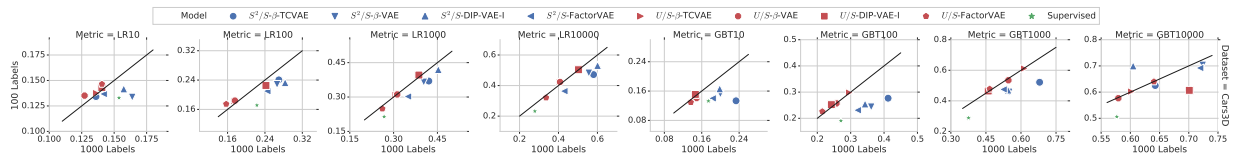


Figure 5: Comparison of the median downstream performance after validation with 100 vs. 1000 examples on Cars3D. The downstream tasks are: cross-validated Logistic Regression (LR) and Gradient Boosting classifier (GBT) both trained with 10, 100, 1000 and 10 000 examples.

sizes for this downstream task: 10, 100, 1000 and 10 000 samples. We train the same cross-validated logistic regression and gradient boosting classifier as used in [42]. In Figure 5 we compare for each method the median downstream performance after validation with 100 vs. 1000 examples. We observe that, depending on the data set and number of samples used for the downstream task, having more labels upstream can improve downstream performance of S^2/S methods. Furthermore, one can see from the results obtained for the fully supervised baseline that training without the unsupervised loss can significantly harm performance. Finally, we observe in Figure 4 (right) that S^2/S methods often outperform U/S in downstream performance.

Conclusions: The results presented in this section lead us to conclude that finding sample efficient disentanglement metrics is an important research direction for practical applications of disentanglement. However, if sufficiently large amounts of labeled data are available, it seems better to use some of the labels during training and rely on a regular train/validation split for model selection. Finding robust and efficient semi-supervised methods is thus also a research direction that should be explored, especially when weaker forms of supervision are available.

4.3 How robust is semi-supervised training to imprecise labels?

In this section, we explore the effect of binning the labels used in the S^2/S methods and how it compares to binning the labels in U/S methods. In Figure 6 (right) we observe that binning does not significantly worsen the performance of both the supervised validation and the semi-supervised training. Sometimes the regularization induced by simplifying the labels actually appears to improve generalization due to a reduction in overfitting. Comparing Figure 6 (left) and (center), we observe that the model selection metrics are slightly more robust than the semi-supervised loss especially when only 100 labeled examples are available. However, the semi-supervised approaches still outperform supervised model selection in 64.8% of the cases (with 100 examples) even with binned labels.

Conclusion: These results show that not only U/S methods based on sample efficient disentanglement metrics but also S^2/S methods are robust to imprecise observations of \mathbf{z} .

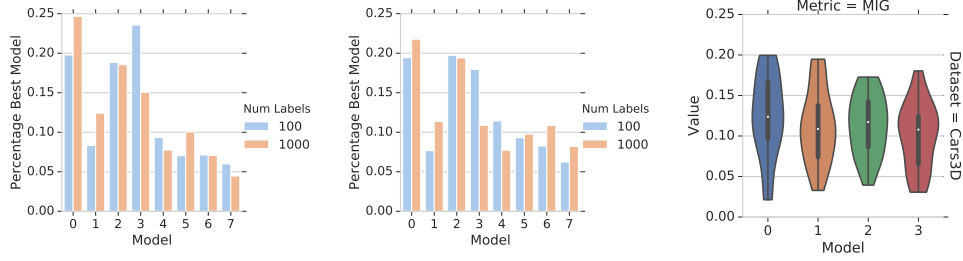


Figure 6: Probability of each method being the best on a random test metric and a random data set after validation on perfect labels (left) and binned labels (center). Legend: 0= S^2/S - β -TCVAE, 1= S^2/S - β -VAE, 2= S^2/S -DIP-VAE-I, 3= S^2/S -FactorVAE, 4= U/S - β -TCVAE, 5= U/S - β -VAE, 6= U/S -DIP-VAE-I, 7= U/S -FactorVAE. For the U/S methods we sample the validation metric uniformly. (right) Distribution of models trained with perfect and binned labels with 100 samples, U/S validated with MIG. Legend: U/S with perfect (Model 0) and binned labels (Model 1). S^2/S with perfect (Model 2) and binned labels (Model 3).

4.4 Ordering as an inductive bias

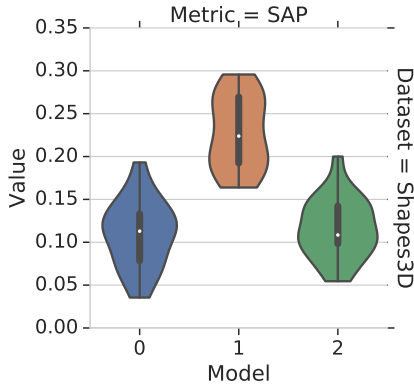


Figure 7: Violin plot showing the effect of removing the inductive bias given by the ordering of the labels on semi-supervised methods. Models are abbreviated as: 0= U/S with perfect labels, 1= S^2/S with perfect labels, 2= S^2/S training with permuted labels.

In this section, we verify that the supervised regularizer we considered relies on the inductive bias given by the ordinal information present in the labels. Note that all the continuous factors of variation are binned in the considered data sets. We analyze how much the performance of the semi-supervised approach degrades when the ordering information is removed. For this reason, we permute the order of the values of the factors of variation. Note that after removing the ordering information the supervised loss will still be at its minimum if $r(\mathbf{x})$ matches \mathbf{z} . However, the ordering information is now useless and potentially detrimental as it does not reflect the natural ordering of the true generative factors. We also remark that none of the disentanglement metrics make use of the ordinal information, so the performance degradation cannot be explained by fitting the wrong labels. In Figure 7, we observe that the S^2/S approaches heavily rely on the ordering information and removing it significantly harms the performances of the test disentanglement metrics regardless of the fact that they are blind to ordering.

Conclusions: Imposing a suitable inductive bias (ordinal structure) on the ground-truth generative model in the form of a supervised regularizer is useful for disentanglement

if its assumptions are correct. If the assumptions are violated, there is no benefit anymore over unsupervised training with supervised model selection (which is invariant to the ordinal structure).

5 Conclusion

In this paper, we investigated whether a very small number of labels can be used to reliably learn disentangled representations. We found that existing disentanglement metrics can in fact be used to perform model selection on models trained in a completely unsupervised fashion even when the labels are few and imprecise. We further showed that one can obtain even better results if one incorporates the labels and inductive biases on the factors of variation (such as ordering) into the learning process using a simple supervised regularizer. In our opinion, these results provide the basis for further work in this setting: Different supervised regularizers should be explored, aiming to regularize towards a different type of structure in the latent space, and/or aiming to impose different inductive biases. Similarly, one could design different model selection techniques, for example by designing novel disentanglement metrics that work well in the regime where few labels are available. Finally, differentiable disentanglement metrics should be developed that could be used in both scenarios.

Acknowledgements

This research was partially supported by the Max Planck ETH Center for Learning Systems and by an ETH core grant (to Gunnar Rätsch). This work was partially done while Francesco Locatello was at Google Research Zurich.

References

- [1] Francis Bach and Michael Jordan. Kernel independent component analysis. *Journal of Machine Learning Research*, 3(7):1–48, 2002.
- [2] Yoshua Bengio, Aaron Courville, and Pascal Vincent. Representation learning: A review and new perspectives. *IEEE Transactions on Pattern Analysis and Machine Intelligence*, 35(8):1798–1828, 2013.
- [3] Yoshua Bengio, Yann LeCun, et al. Scaling learning algorithms towards AI. *Large-scale Kernel Machines*, 34(5):1–41, 2007.
- [4] Diane Bouchacourt, Ryota Tomioka, and Sebastian Nowozin. Multi-level variational autoencoder: Learning disentangled representations from grouped observations. In *AAAI Conference on Artificial Intelligence*, 2018.
- [5] Christopher P Burgess, Irina Higgins, Arka Pal, Loic Matthey, Nick Watters, Guillaume Desjardins, and Alexander Lerchner. Understanding disentangling in beta-VAE. *arXiv preprint arXiv:1804.03599*, 2018.
- [6] Tian Qi Chen, Xuechen Li, Roger Grosse, and David Duvenaud. Isolating sources of disentanglement in variational autoencoders. In *Advances in Neural Information Processing Systems*, 2018.
- [7] Xi Chen, Yan Duan, Rein Houthoofd, John Schulman, Ilya Sutskever, and Pieter Abbeel. Infogan: Interpretable representation learning by information maximizing generative adversarial nets. In *Advances in Neural Information Processing Systems*, 2016.
- [8] Brian Cheung, Jesse A Livezey, Arjun K Bansal, and Bruno A Olshausen. Discovering hidden factors of variation in deep networks. *arXiv preprint arXiv:1412.6583*, 2014.
- [9] Taco Cohen and Max Welling. Learning the irreducible representations of commutative lie groups. In *International Conference on Machine Learning*, 2014.
- [10] Pierre Comon. Independent component analysis, a new concept? *Signal Processing*, 36(3):287–314, 1994.
- [11] Alexander D’Amour. On multi-cause approaches to causal inference with unobserved confounding: Two cautionary failure cases and a promising alternative. In *International Conference on Artificial Intelligence and Statistics*, 2019.
- [12] Zhiwei Deng, Rajitha Navarathna, Peter Carr, Stephan Mandt, Yisong Yue, Iain Matthews, and Greg Mori. Factorized variational autoencoders for modeling audience reactions to movies. In *IEEE Conference on Computer Vision and Pattern Recognition*, 2017.
- [13] Emily L Denton and Vighnesh Birodkar. Unsupervised learning of disentangled representations from video. In *Advances in Neural Information Processing Systems*, 2017.
- [14] Cian Eastwood and Christopher KI Williams. A framework for the quantitative evaluation of disentangled representations. In *International Conference on Learning Representations*, 2018.
- [15] Vincent Fortuin, Matthias Hüser, Francesco Locatello, Heiko Strathmann, and Gunnar Rätsch. Deep self-organization: Interpretable discrete representation learning on time series. In *International Conference on Learning Representations*. 2019.
- [16] Marco Fraccaro, Simon Kamronn, Ulrich Paquet, and Ole Winther. A disentangled recognition and nonlinear dynamics model for unsupervised learning. In *Advances in Neural Information Processing Systems*, 2017.
- [17] Ian Goodfellow, Honglak Lee, Quoc V Le, Andrew Saxe, and Andrew Y Ng. Measuring invariances in deep networks. In *Advances in Neural Information Processing Systems*, 2009.
- [18] Ross Goroshin, Michael F Mathieu, and Yann LeCun. Learning to linearize under uncertainty. In *Advances in Neural Information Processing Systems*, 2015.

- [19] Irina Higgins, David Amos, David Pfau, Sebastien Racaniere, Loic Matthey, Danilo Rezende, and Alexander Lerchner. Towards a definition of disentangled representations. *arXiv preprint arXiv:1812.02230*, 2018.
- [20] Irina Higgins, Loic Matthey, Arka Pal, Christopher Burgess, Xavier Glorot, Matthew Botvinick, Shakir Mohamed, and Alexander Lerchner. beta-VAE: Learning basic visual concepts with a constrained variational framework. In *International Conference on Learning Representations*, 2017.
- [21] Irina Higgins, Arka Pal, Andrei Rusu, Loic Matthey, Christopher Burgess, Alexander Pritzel, Matthew Botvinick, Charles Blundell, and Alexander Lerchner. Darla: Improving zero-shot transfer in reinforcement learning. In *International Conference on Machine Learning*, 2017.
- [22] Irina Higgins, Nicolas Sonnerat, Loic Matthey, Arka Pal, Christopher P Burgess, Matko Bošnjak, Murray Shanahan, Matthew Botvinick, Demis Hassabis, and Alexander Lerchner. Scan: Learning hierarchical compositional visual concepts. In *International Conference on Learning Representations*, 2018.
- [23] Geoffrey E Hinton, Alex Krizhevsky, and Sida D Wang. Transforming auto-encoders. In *International Conference on Artificial Neural Networks*, 2011.
- [24] Jun-Ting Hsieh, Bingbin Liu, De-An Huang, Li F Fei-Fei, and Juan Carlos Nieves. Learning to decompose and disentangle representations for video prediction. In *Advances in Neural Information Processing Systems*, 2018.
- [25] Wei-Ning Hsu, Yu Zhang, and James Glass. Unsupervised learning of disentangled and interpretable representations from sequential data. In *Advances in Neural Information Processing Systems*, 2017.
- [26] Aapo Hyvarinen and Hiroshi Morioka. Unsupervised feature extraction by time-contrastive learning and nonlinear ica. In *Advances in Neural Information Processing Systems*, 2016.
- [27] Aapo Hyvärinen and Petteri Pajunen. Nonlinear independent component analysis: Existence and uniqueness results. *Neural Networks*, 1999.
- [28] Aapo Hyvarinen, Hiroaki Sasaki, and Richard E Turner. Nonlinear ica using auxiliary variables and generalized contrastive learning. In *International Conference on Artificial Intelligence and Statistics*, 2019.
- [29] Christian Jutten and Juha Karhunen. Advances in nonlinear blind source separation. In *International Symposium on Independent Component Analysis and Blind Signal Separation*, pages 245–256, 2003.
- [30] Theofanis Karaletsos, Serge Belongie, and Gunnar Rätsch. Bayesian representation learning with oracle constraints. *arXiv preprint arXiv:1506.05011*, 2015.
- [31] Hyunjik Kim and Andriy Mnih. Disentangling by factorising. In *International Conference on Machine Learning*, 2018.
- [32] Diederik P Kingma, Shakir Mohamed, Danilo Jimenez Rezende, and Max Welling. Semi-supervised learning with deep generative models. In *Advances in Neural Information Processing Systems*, 2014.
- [33] Diederik P Kingma and Max Welling. Auto-encoding variational Bayes. In *International Conference on Learning Representations*, 2014.
- [34] Jack Klys, Jake Snell, and Richard Zemel. Learning latent subspaces in variational autoencoders. In *Advances in Neural Information Processing Systems*. 2018.
- [35] Tejas D Kulkarni, William F Whitney, Pushmeet Kohli, and Josh Tenenbaum. Deep convolutional inverse graphics network. In *Advances in Neural Information Processing Systems*, 2015.
- [36] Abhishek Kumar, Prasanna Sattigeri, and Avinash Balakrishnan. Variational inference of disentangled latent concepts from unlabeled observations. In *International Conference on Learning Representations*, 2018.
- [37] Brenden M Lake, Tomer D Ullman, Joshua B Tenenbaum, and Samuel J Gershman. Building machines that learn and think like people. *Behavioral and Brain Sciences*, 40, 2017.
- [38] Adrien Laversanne-Finot, Alexandre Pere, and Pierre-Yves Oudeyer. Curiosity driven exploration of learned disentangled goal spaces. In *Conference on Robot Learning*, 2018.

- [39] Yann LeCun, Yoshua Bengio, and Geoffrey Hinton. Deep learning. *Nature*, 521(7553):436, 2015.
- [40] Yann LeCun, Fu Jie Huang, and Leon Bottou. Learning methods for generic object recognition with invariance to pose and lighting. In *IEEE Conference on Computer Vision and Pattern Recognition*, 2004.
- [41] Karel Lenc and Andrea Vedaldi. Understanding image representations by measuring their equivariance and equivalence. In *IEEE Conference on Computer Vision and Pattern Recognition*, 2015.
- [42] Francesco Locatello, Stefan Bauer, Mario Lucic, Sylvain Gelly, Bernhard Schölkopf, and Olivier Bachem. Challenging common assumptions in the unsupervised learning of disentangled representations. In *(To appear) International Conference on Machine Learning*, 2019.
- [43] Francesco Locatello, Damien Vincent, Ilya Tolstikhin, Gunnar Rätsch, Sylvain Gelly, and Bernhard Schölkopf. Competitive training of mixtures of independent deep generative models. In *Workshop at the 6th International Conference on Learning Representations (ICLR)*, 2018.
- [44] Emile Mathieu, Tom Rainforth, N. Siddharth, and Yee Whye Teh. Disentangling disentanglement in variational auto-encoders. *arXiv preprint arXiv:1812.02833*, 2018.
- [45] Michael F Mathieu, Junbo J Zhao, Aditya Ramesh, Pablo Sprechmann, and Yann LeCun. Disentangling factors of variation in deep representation using adversarial training. In *Advances in Neural Information Processing Systems*, 2016.
- [46] Ashvin V Nair, Vitchyr Pong, Murtaza Dalal, Shikhar Bahl, Steven Lin, and Sergey Levine. Visual reinforcement learning with imagined goals. In *Advances in Neural Information Processing Systems*, 2018.
- [47] Siddharth Narayanaswamy, T Brooks Paige, Jan-Willem Van de Meent, Alban Desmaison, Noah Goodman, Pushmeet Kohli, Frank Wood, and Philip Torr. Learning disentangled representations with semi-supervised deep generative models. In *Advances in Neural Information Processing Systems*, 2017.
- [48] Judea Pearl. *Causality*. Cambridge University Press, 2009.
- [49] Jonas Peters, Dominik Janzing, and Bernhard Schölkopf. *Elements of Causal Inference - Foundations and Learning Algorithms*. Adaptive Computation and Machine Learning Series. MIT Press, 2017.
- [50] Scott Reed, Kihyuk Sohn, Yuting Zhang, and Honglak Lee. Learning to disentangle factors of variation with manifold interaction. In *International Conference on Machine Learning*, 2014.
- [51] Scott Reed, Yi Zhang, Yuting Zhang, and Honglak Lee. Deep visual analogy-making. In *Advances in Neural Information Processing Systems*, 2015.
- [52] Karl Ridgeway and Michael C Mozer. Learning deep disentangled embeddings with the f-statistic loss. In *Advances in Neural Information Processing Systems*, 2018.
- [53] Michal Rolínek, Dominik Zietlow, and Georg Martius. Variational autoencoders recover pca directions (by accident). In *Proceedings IEEE Conf. on Computer Vision and Pattern Recognition*, 2019.
- [54] P. K. Rubenstein, B. Schölkopf, and I. Tolstikhin. Learning disentangled representations with wasserstein auto-encoders. In *Workshop at the 6th International Conference on Learning Representations (ICLR)*, 2018.
- [55] Adrià Ruiz, Oriol Martinez, Xavier Binefa, and Jakob Verbeek. Learning disentangled representations with reference-based variational autoencoders. *arXiv preprint arXiv:1901.08534*, 2019.
- [56] Jürgen Schmidhuber. Learning factorial codes by predictability minimization. *Neural Computation*, 4(6):863–879, 1992.
- [57] Bernhard Schölkopf, Dominik Janzing, Jonas Peters, Eleni Sgouritsa, Kun Zhang, and Joris Mooij. On causal and anticausal learning. In *International Conference on Machine Learning*, 2012.
- [58] P. Spirtes, C. Glymour, and R. Scheines. *Causation, prediction, and search*. MIT Press, 2000.

- [59] Xander Steenbrugge, Sam Leroux, Tim Verbelen, and Bart Dhoedt. Improving generalization for abstract reasoning tasks using disentangled feature representations. In *Workshop on Relational Representation Learning at NeurIPS*, 2018.
- [60] Raphael Suter, Djordje Miladinović, Stefan Bauer, and Bernhard Schölkopf. Interventional robustness of deep latent variable models, 2019.
- [61] Valentin Thomas, Emmanuel Bengio, William Fedus, Jules Pondard, Philippe Beaudoin, Hugo Larochelle, Joelle Pineau, Doina Precup, and Yoshua Bengio. Disentangling the independently controllable factors of variation by interacting with the world. *Learning Disentangled Representations Workshop at NeurIPS*, 2017.
- [62] Michael Tschannen, Olivier Bachem, and Mario Lucic. Recent advances in autoencoder-based representation learning. *arXiv preprint arXiv:1812.05069*, 2018.
- [63] William F Whitney, Michael Chang, Tejas Kulkarni, and Joshua B Tenenbaum. Understanding visual concepts with continuation learning. *arXiv preprint arXiv:1602.06822*, 2016.
- [64] Jimei Yang, Scott E Reed, Ming-Hsuan Yang, and Honglak Lee. Weakly-supervised disentangling with recurrent transformations for 3D view synthesis. In *Advances in Neural Information Processing Systems*, 2015.
- [65] Li Yingzhen and Stephan Mandt. Disentangled sequential autoencoder. In *International Conference on Machine Learning*, 2018.

Table 1: Encoder and Decoder architecture for the main experiment.

Encoder	Decoder
Input: $64 \times 64 \times \text{number of channels}$	Input: \mathbb{R}^{10}
4×4 conv, 32 ReLU, stride 2	FC, 256 ReLU
4×4 conv, 32 ReLU, stride 2	FC, $4 \times 4 \times 64$ ReLU
4×4 conv, 64 ReLU, stride 2	4×4 upconv, 64 ReLU, stride 2
4×4 conv, 64 ReLU, stride 2	4×4 upconv, 32 ReLU, stride 2
FC 256, FC 2×10	4×4 upconv, 32 ReLU, stride 2
	4×4 upconv, number of channels, stride 2

Table 2: Hyperparameters explored for the different disentanglement methods.

Model	Parameter	Values
β -VAE	β	[1, 2, 4, 6, 8, 16]
S^2/S β -VAE	β	[1, 2, 4, 6, 8, 16]
	γ_{sup}	[1, 2, 4, 6, 8, 16]
FactorVAE	γ	[10, 20, 30, 40, 50, 100]
S^2/S FactorVAE	γ	[10, 20, 30, 40, 50, 100]
	γ_{sup}	[10, 20, 30, 40, 50, 100]
DIP-VAE-I	λ_{od}	[1, 2, 5, 10, 20, 50]
	λ_d	$10\lambda_{od}$
S^2/S DIP-VAE-I	λ_{od}	[1, 2, 5, 10, 20, 50]
	λ_d	$10\lambda_{od}$
	γ_{sup}	[1, 2, 5, 10, 20, 50]
β -TCVAE	β	[1, 2, 4, 6, 8, 10]
S^2/S β -TCVAE	β	[1, 2, 4, 6, 8, 10]
	γ_{sup}	[1, 2, 4, 6, 8, 10]

A Architectures and detailed experimental design

The architecture shared across every method is the default one in the `disentanglement_lib` which we describe here for completeness in Table 1 along with the other fixed hyperparameters in Table 3a and the discriminator for total correlation estimation in FactorVAE Table 3b with hyperparameters in Table 3c. The hyperparameters that were swept for the different methods can be found in Table 2. All the hyperparameters for which we report single values were not varied and are selected based on the literature.

B Detailed plots for Section 3

In Figure 8, we compute the rank correlation between the validation metrics computed on 100 samples and the test metrics on each data set. In Figure 9, we observe that the correlation improves if we consider 1000 labeled examples. These plots are the extended version of Figure 2 showing the results on all data sets.

In Figure 10, we plot for each unsupervised model its validation MIG with 100 samples against the DCI test score on dSprites. We can see that indeed there is a strong linear relationship.

Figures 11 and 12 show the rank correlation between the validation metrics with binned values and the test metrics with exact labels. These plots are the extended version of Figure 3 showing the results on all data sets.

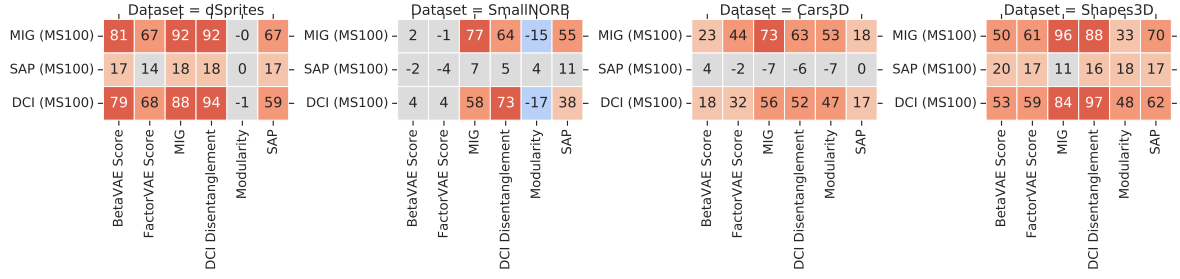


Figure 8: Rank correlation of validation metrics computed with 100 examples and test metrics on each data set.

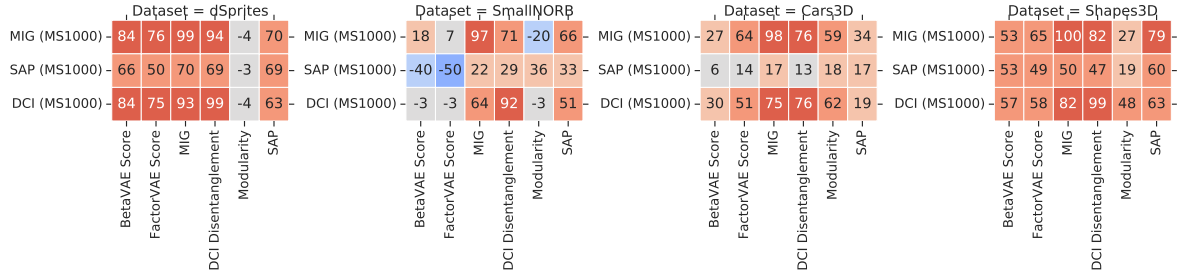


Figure 9: Rank correlation of validation metrics computed with 1000 examples and test metrics on each data set.

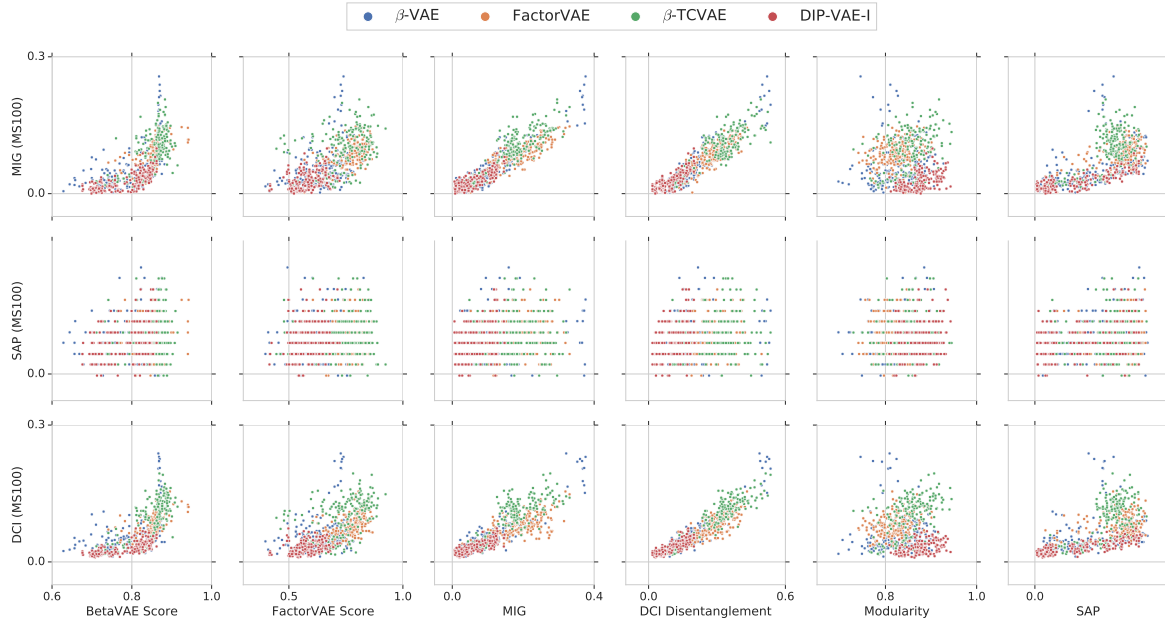


Figure 10: Scatter plot of validation and test metrics on dSprites before model selection. The validation metrics are computed with 100 examples.

Table 3: Other fixed hyperparameters.

(a) Hyperparameters common to all considered methods.

Parameter	Values
Batch size	64
Latent space dimension	10
Optimizer	Adam
Adam: beta1	0.9
Adam: beta2	0.999
Adam: epsilon	1e-8
Adam: learning rate	0.0001
Decoder type	Bernoulli
Training steps	300000

(b) Architecture for the discriminator in FactorVAE.

Discriminator
FC, 1000 leaky ReLU
FC, 1000 leaky ReLU
FC, 1000 leaky ReLU
FC, 1000 leaky ReLU
FC, 1000 leaky ReLU
FC, 1000 leaky ReLU
FC, 2

(c) Parameters for the discriminator in FactorVAE.

Parameter	Values
Batch size	64
Optimizer	Adam
Adam: beta1	0.5
Adam: beta2	0.9
Adam: epsilon	1e-8
Adam: learning rate	0.0001

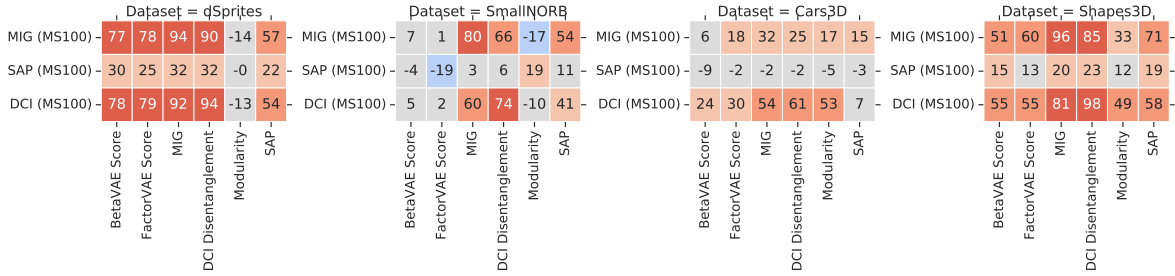


Figure 11: Rank correlation of validation metrics and test metrics. Validation metrics are computed with 100 examples with *labels binned to five categories*.

C Detailed plots for Section 4

C.1 Does supervision help training?

In Figure 15 we plot the median of each score across the draws of the labeled subset achieved by the best models on each data set (using 100 vs 1000 examples). For the U/S models we use MIG for validation (MIG has a higher rank correlation with most of the testing metric than other validation metrics, see Figure 2). This plot extends Figure 4 (left) to all data set and test score.

In Table 4, we compute how often each S^2/S method outperforms the corresponding U/S on a random disentanglement metric and data set. We observe that S^2/S often outperforms U/S , especially when more labels are available.

In Figure 13 can be observed that with 1000 samples the semi-supervised method is often better than the corresponding U/S even using the test MIG computed with 10 000 samples for validation. We conclude that the semi-supervised loss improves the training and transfer better to different metrics

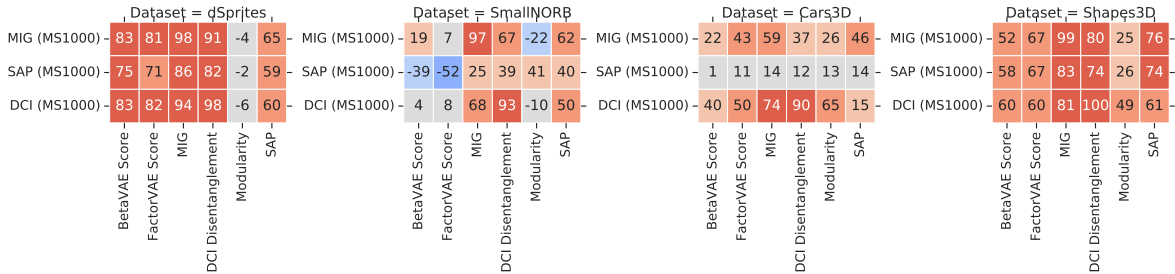


Figure 12: Rank correlation of validation metrics and test metrics. Validation metrics are computed with 1000 examples with *labels binned to five categories*.

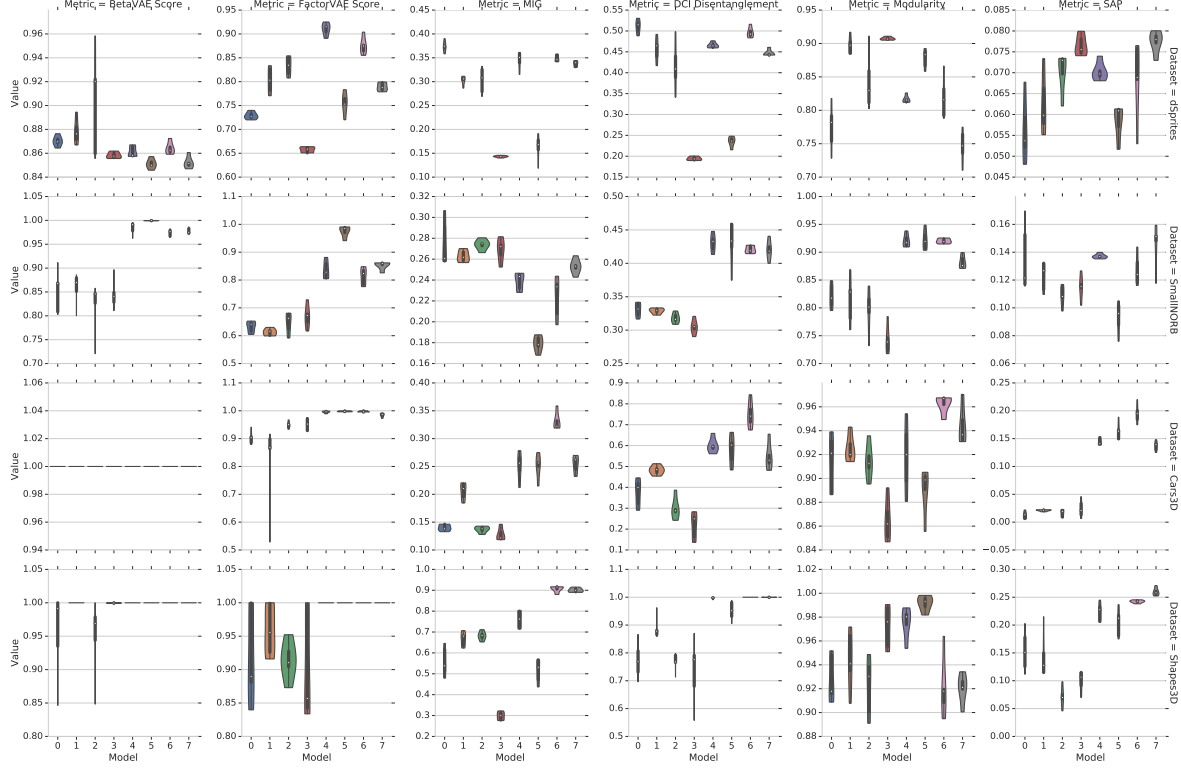


Figure 13: Test scores of the U/S methods using the test MIG as validation and the S^2/S models with 1000 labeled examples. Legend: 0= U/S - β -VAE, 1= U/S - β -TCVAE, 2= U/S -FactorVAE, 3= U/S -DIP-VAE-I, 4= S^2/S - β -VAE, 5= S^2/S -DIP-VAE-I, 6= S^2/S - β -TCVAE, 7= S^2/S -FactorVAE

Method	Type	SAP 100	SAP 1000	MIG 100	MIG 1000	DCI 100	DCI 1000
β -VAE	S^2/S	72.6%	79.2%	53.9%	74.2%	53.9%	69.2%
	U/S	27.4%	20.8%	46.1%	25.8%	46.1%	30.8%
FactorVAE	S^2/S	71.5%	79.4%	64.5%	75.2%	68.5%	77.6%
	U/S	28.5%	20.6%	35.5%	24.8%	31.5%	22.4%
β -TCVAE	S^2/S	79.5%	80.6%	58.5%	75.0%	62.9%	74.4%
	U/S	20.5%	19.4%	41.5%	25.0%	37.1%	25.6%
DIP-VAE-I	S^2/S	81.6%	83.5%	64.9%	74.8%	67.7%	70.5%
	U/S	18.4%	16.5%	35.1%	25.2%	32.3%	29.5%

Table 4: Percentage of how often S^2/S improves upon U/S on for each approach separately. The standard deviation is between 3% and 5% and can be computed as $\sqrt{p(1-p)/120}$.

than the MIG. In Figure 14, we observe similar trends if we use the test DCI Disentanglement with 10 000 samples for validation of the U/S methods.

in Figure 16 we observe that increasing the supervised regularization makes that the matrix holding the mutual information between all pairs of entries of \mathbf{z} and $r(\mathbf{x})$ closer to diagonal. This plots extend Figure 4 to all data sets.

In Figure 17 we compare the median downstream performance after validation with 100 vs 1000 samples. This plot extends Figure 5 to all data sets. Finally, we observe in Table 5 that semi-supervised methods often outperforms U/S in downstream performance, especially when more labels are available.

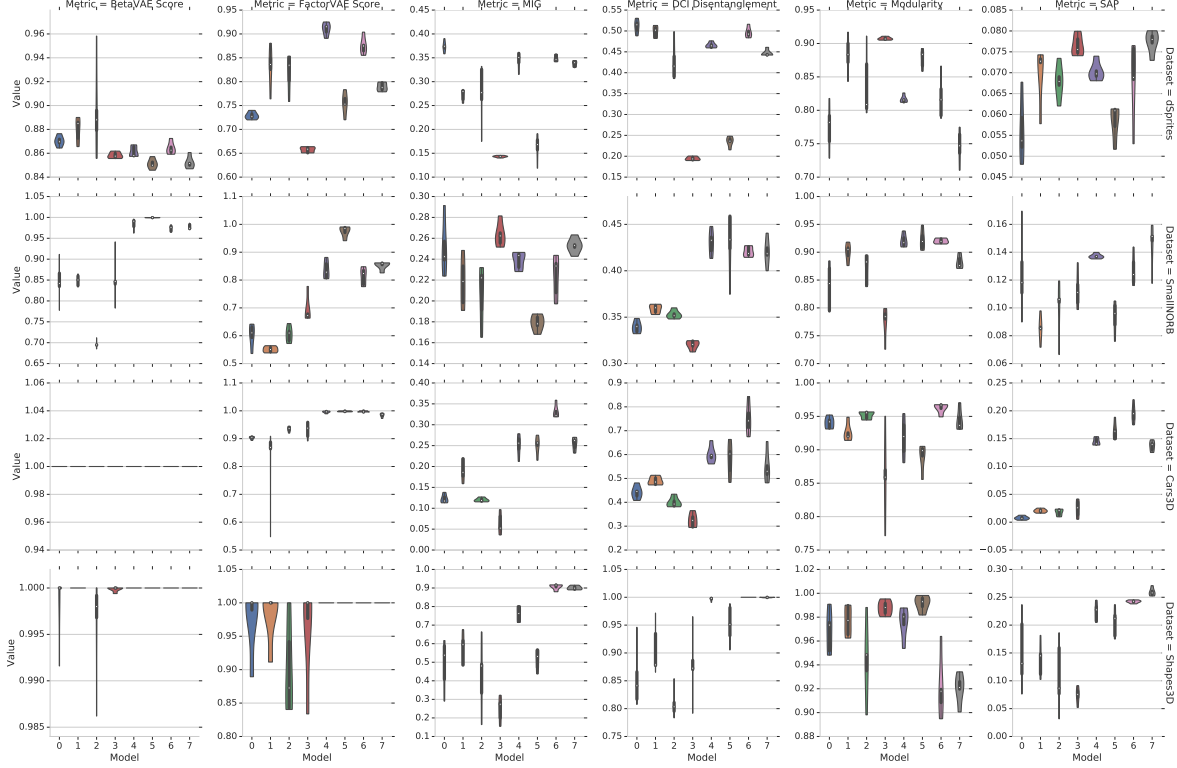


Figure 14: Test scores of the U/S methods using the test DCI as validation and the S^2/S models with 1000 labeled examples. Legend: 0= U/S - β -VAE, 1= U/S - β -TCVAE, 2= U/S -FactorVAE, 3= U/S -DIP-VAE-I, 4= S^2/S - β -VAE, 5= S^2/S -DIP-VAE-I, 6= S^2/S - β -TCVAE, 7= S^2/S -FactorVAE

Method	Type	SAP 100	SAP 1000	MIG 100	MIG 1000	DCI 100	DCI 1000
β -VAE	S^2/S	70.0%	75.6%	53.8%	75.0%	43.8%	71.9%
	U/S	30.0%	24.4%	46.2%	25.0%	56.2%	28.1%
FactorVAE	S^2/S	61.2%	71.9%	62.5%	78.1%	63.8%	71.2%
	U/S	38.8%	28.1%	37.5%	21.9%	36.2%	28.8%
β -TCVAE	S^2/S	70.6%	72.7%	51.9%	71.9%	55.6%	67.5%
	U/S	29.4%	27.3%	48.1%	28.1%	44.4%	32.5%
DIP-VAE-I	S^2/S	71.9%	80.6%	50.6%	75.6%	50.6%	65.0%
	U/S	28.1%	19.4%	49.4%	24.4%	49.4%	35.0%

Table 5: Percentage of how often S^2/S improves upon U/S on the downstream performance. The standard deviation is between 3% and 4% and can be computed as $\sqrt{p(1-p)/160}$.

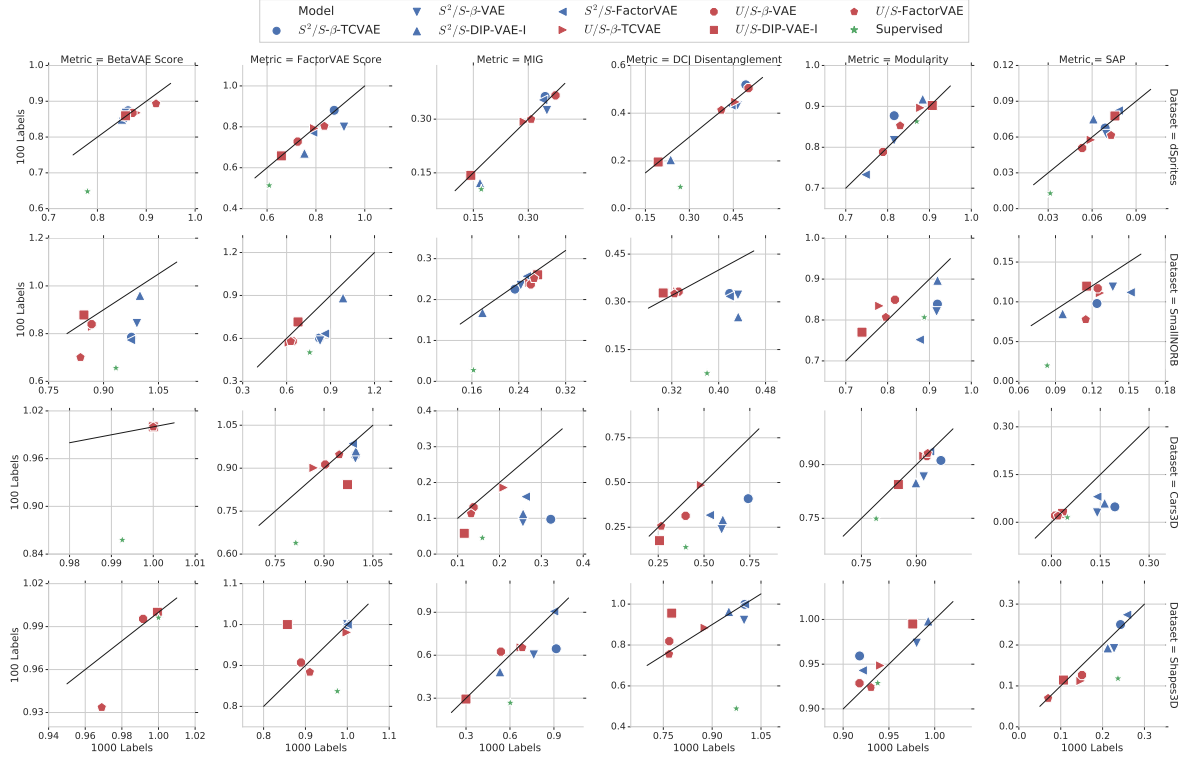


Figure 15: Median across the draws of the labeled data set of the test scores on each data set after validation with 100 and 1000 labeled examples. U/S were validated with the MIG.

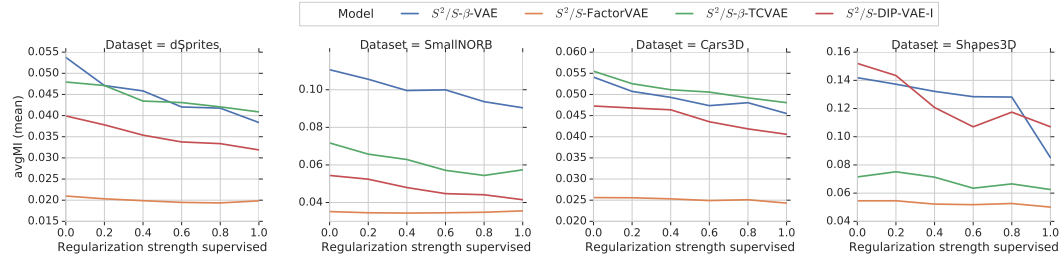


Figure 16: Increasing the supervised regularization strength makes the matrix of pairwise mutual information $I(\mathbf{z}, r(\mathbf{x}))$ closer to diagonal.

C.2 What happens if we collect imprecise labels?

In Figures 18 and 19 we observe that binning does not significantly worsen the performance of both the supervised validation and the semi-supervised training. These plots extend Figure 6 (right) to both sample sizes, all test scores and data sets.

In Table 6 we show how often each S^2/S method outperforms the corresponding U/S on a random disentanglement metric and data set with binned labels.

C.3 Ordering as inductive bias

In Figure 20, we extend Figure 7 to all test scores and data sets.

In Table 7 we compute how often each S^2/S method outperforms the corresponding U/S on a random disentanglement metric and data set with binned labels. We observe that in this case U/S is superior most of the times but the gap reduces with more labels.

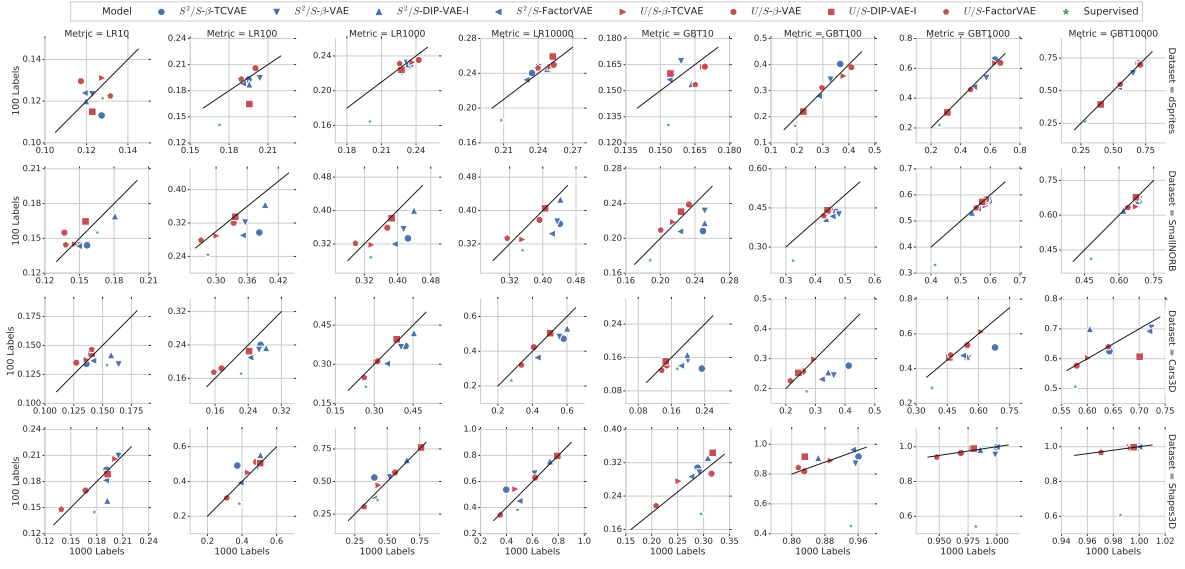


Figure 17: Comparison of the median downstream performance after validation with 100 vs. 1000 examples on each data set. The downstream tasks are: cross-validated Logistic Regression (LR) and Gradient Boosting classifier (GBT) both trained with 10, 100, 1000 and 10 000 examples.

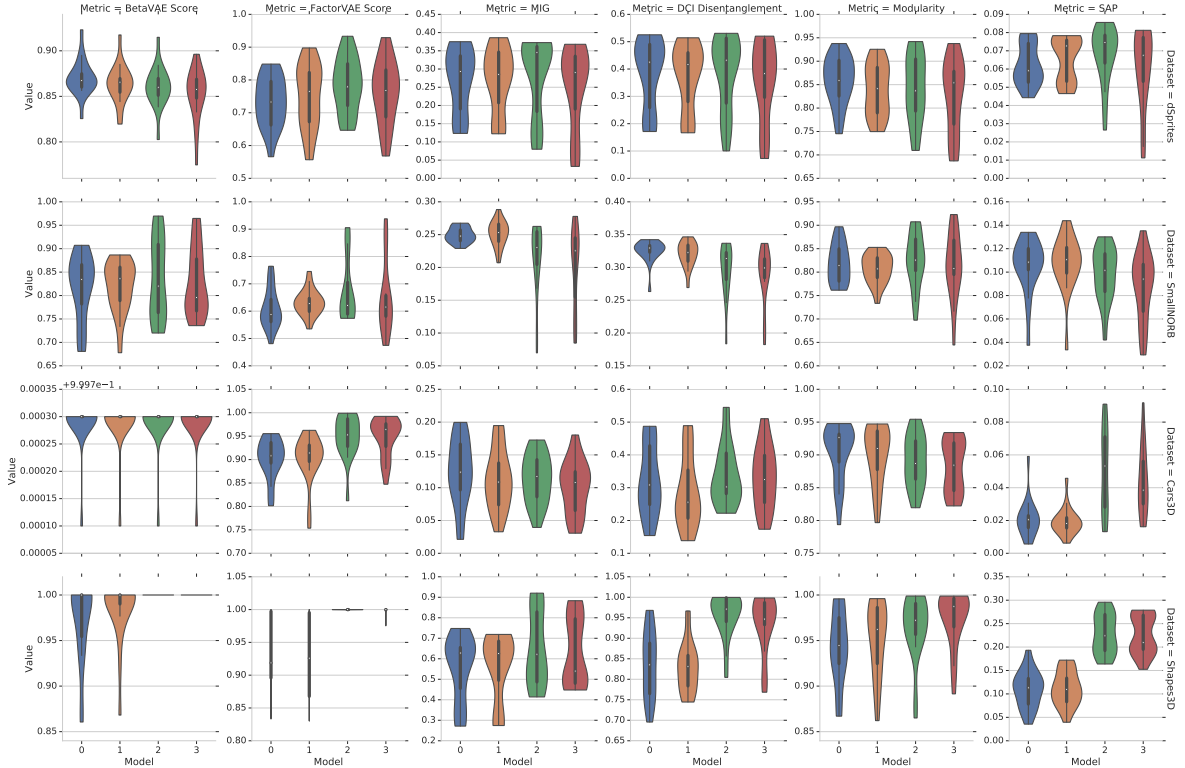


Figure 18: Distribution of models trained with perfect and binned labels with 100 samples, U/S validated with MIG. Legend: U/S with perfect (Model 0) and binned labels (Model 1). S^2/S with perfect (Model 2) and binned labels (Model 3).

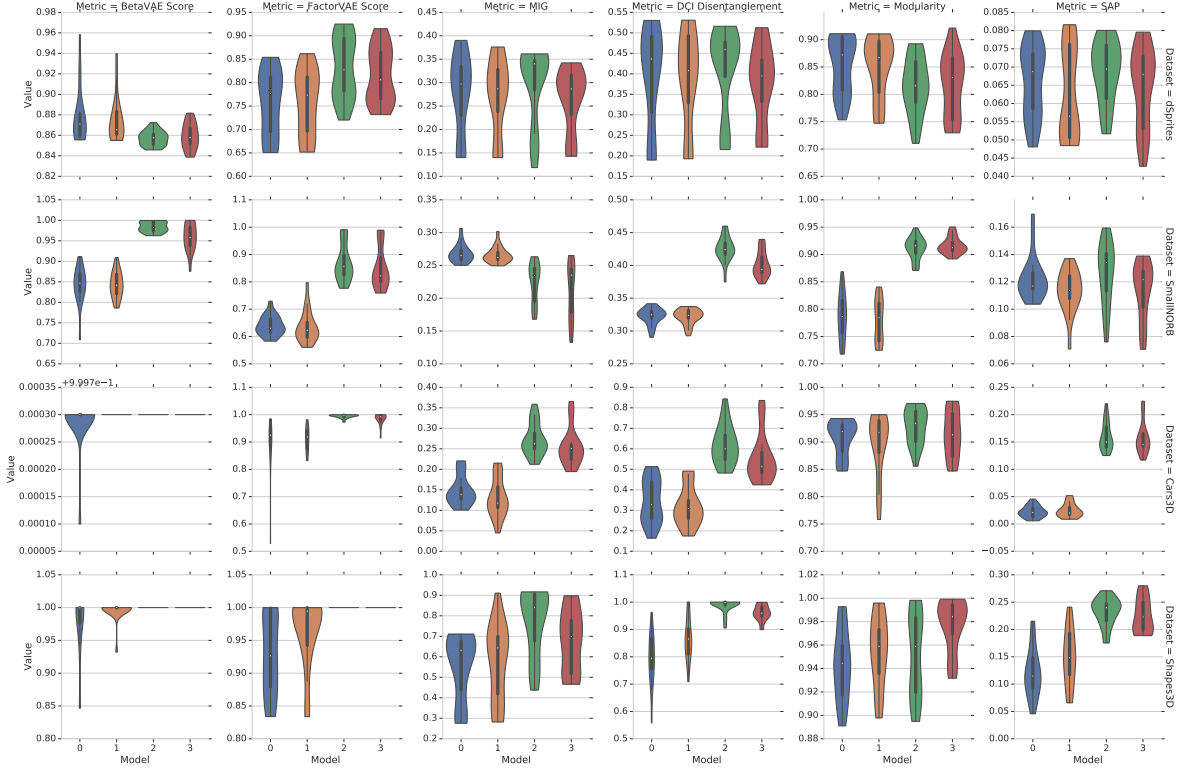


Figure 19: Distribution of models trained with perfect and binned labels with 1000 samples, U/S validated with MIG. Legend: U/S with perfect (Model 0) and binned labels (Model 1). S^2/S with perfect (Model 2) and binned labels (Model 3).

Method	Type	SAP 100	SAP 1000	MIG 100	MIG 1000	DCI 100	DCI 1000
β -VAE	S^2/S	66.9%	76.3%	50.4%	75.2%	44.5%	74.6%
	U/S	33.1%	23.7%	49.6%	24.8%	55.5%	25.4%
FactorVAE	S^2/S	72.4%	67.9%	60.5%	63.2%	56.8%	62.4%
	U/S	27.6%	32.1%	39.5%	36.8%	43.2%	37.6%
β -TCVAE	S^2/S	79.2%	77.9%	58.5%	74.0%	61.2%	72.7%
	U/S	20.8%	22.1%	41.5%	26.0%	38.8%	27.3%
DIP-VAE-I	S^2/S	67.7%	75.8%	57.4%	71.8%	53.4%	69.6%
	U/S	32.3%	24.2%	42.6%	28.2%	46.6%	30.4%

Table 6: Percentage of how often S^2/S improves upon U/S for each method on a random disentanglement score and data set with binned labels. The standard deviation is between 3% and 5% and can be computed as $\sqrt{p(1-p)/120}$.

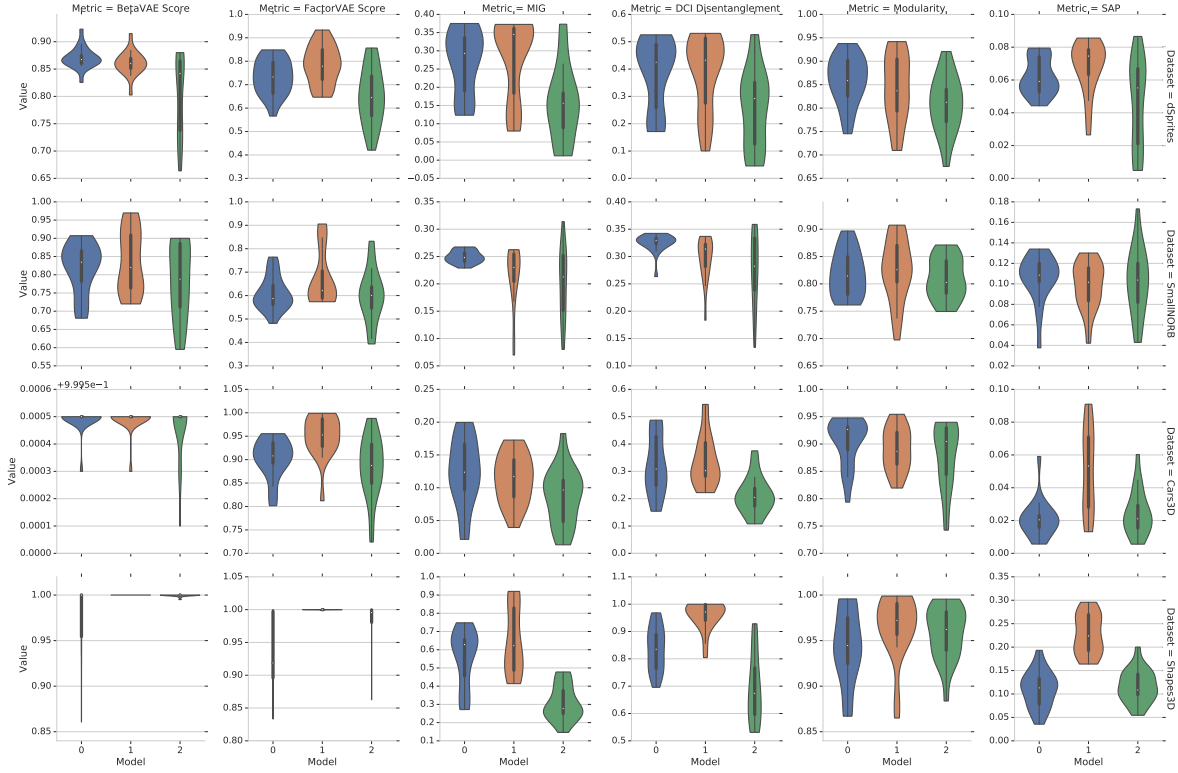


Figure 20: Violin plot showing the effect of removing the inductive bias given by the ordering of the labels on semi-supervised methods. Models are abbreviated as: 0= U/S with perfect labels, 1= S^2/S with perfect labels, 2= S^2/S training with permuted labels.

Method	Type	SAP 100	SAP 1000	MIG 100	MIG 1000	DCI 100	DCI 1000
β -VAE	S^2/S permuted	54.8%	55.6%	33.9%	48.0%	34.9%	48.0%
	U/S perfect	45.2%	44.4%	66.1%	52.0%	65.1%	52.0%
FactorVAE	S^2/S permuted	48.0%	44.4%	39.5%	44.4%	41.1%	44.4%
	U/S perfect	52.0%	55.6%	60.5%	55.6%	58.9%	55.6%
β -TCVAE	S^2/S permuted	64.8%	55.5%	34.4%	42.3%	36.8%	43.5%
	U/S perfect	35.2%	44.5%	65.6%	57.7%	63.2%	56.5%
DIP-VAE-I	S^2/S permuted	56.8%	61.9%	30.5%	46.8%	36.4%	46.5%
	U/S perfect	43.2%	38.1%	69.5%	53.2%	63.6%	53.5%

Table 7: Removing the ordering information significantly worsen the performances of the S^2/S on each method. The standard deviation is between 3% and 5% and can be computed as $\sqrt{p(1-p)/120}$.